Large-scale brain simulations on the desktop using procedural connectivity

James C Knight[a,1] **and Thomas Nowotny**[a]

[a]Centre for Computational Neuroscience and Robotics, School of Engineering and Informatics, University of Sussex, Brighton, United Kingdom

Large-scale simulations of spiking neural networks are important for improving our understanding of the dynamics and ultimately function of brains. However, even small mammals such as mice have approximately 1×10^{12} synaptic connections which are typically charaterized by at least one floating point value per synapse. This amounts to several terabytes of connection data – an unrealistic memory requirement for a single desktop machine. Simulations of large spiking neural networks are therefore typically executed on large distributed supercomputers. This is costly and limits large-scale modelling to a select few research groups with the appropriate resources. In this work, we describe extensions to GeNN – our GPU-based spiking neural network simulator – that enable it to 'procedurally' generate connectivity and synaptic weights 'on the go' as spikes are triggered, instead of storing and retrieving them from memory. We find that GPUs are well-suited to this approach because of their raw computational power, which due to memory bandwidth limitations is often under-utilised when simulating spiking neural networks. We demonstrate the value of our approach with a recent model of the Macaque visual cortex consisting of 4.13×10^6 neurons and 24.2×10^9 synapses. Using our new method, this model can be simulated on a single GPU. Our results match those obtained on a supercomputer and the simulation runs faster on a single high-end GPU than a previous simulation executed on over 1000 supercomputer nodes.

spiking neural networks | GPU | high-performance computing | brain simulation

The brain of a mouse has around 70×10^6 neurons, but this number is dwarfed by the 1×10^{12} (1) synapses which connect them. In computer simulations of spiking neural networks, propagating spikes through synapses involves reading a 'row' of synapses connecting a spiking presynaptic neuron to its postsynaptic partners and adding the 'weight' of each synapse in the row to a 'bin' containing the postsynatic neuron's input for the next simulation timestep. Typically, the information describing which neurons are connected by a synapse and with what conductance, is generated before a simulation is run and stored in large matrices in random access memory (RAM). This creates high memory requirements for large-scale brain models, so that they can typically only be simulated on large distributed computer systems using software such as NEST (2) or NEURON (3). By careful design, these simulators can keep the memory requirements for each node constant, even when a simulation is distributed across thousands of nodes (4). However, high performance computer systems are bulky, expensive and consume large amounts of power, meaning that they are typically shared resources that are only accessible to a limited number of researchers and for strongly time-limited investigations.

Neuromorphic systems (5–10) take inspiration from the brain and have been developed specifically for simulating large spiking neural networks. One particular relevant feature of the brain is that its memory elements – the synapses – are co-located with the computing elements – the neurons – throughout the entire system. In neuromorphic systems, this often translates to dedicating a large proportion of each chip to memory. However, while such on-chip memory is fast, it can only be fabricated at relatively low density meaning that many of these systems economize – either by reducing the maximum number of synapses per neuron to as few as 256 or by reducing the precision of the synaptic weights to 6 (10), 4 (5) or even 1 bit (6, 8). Such strategies allow some classes of spiking neural networks to be simulated very efficiently, but reducing the degree of connectivity in large-scale brain simulations to fit within the constraints of current neuromorphic systems inevitably changes their dynamics (11). Unlike the majority of other neuromorphic systems, the SpiNNaker (7) neuromorphic super-computer is entirely programmable and combines a large amount of on-chip memory with external memories, distributed across the system for the storage of synaptic connectivity. SpiNNaker's external memory bandwidth, on-chip memory capacity and the computational power of each core are all tailored to large-scale brain simulation meaning that the output bins of the synapse processing algorithm can fit in on-chip memory and there is enough external memory bandwidth to fetch synaptic rows fast enough for real-time simulation of large-scale models (12). This is a promising approach for future research but, because of its prototype nature, the availability of SpiNNaker hardware is limited and a physically large system is still required for even moderately-sized simulations (9 boards for a simulation with around 10×10^3 neurons and 300×10^6 synapses (12)).

Modern GPUs have relatively small amounts of on-chip memory and, instead, dedicate the majority of their silicon area to arithmetic logic units (ALUs). GPUs use dedictated

www.pnas.org/cgi/doi/10.1073/pnas.XXXXXXXXXX

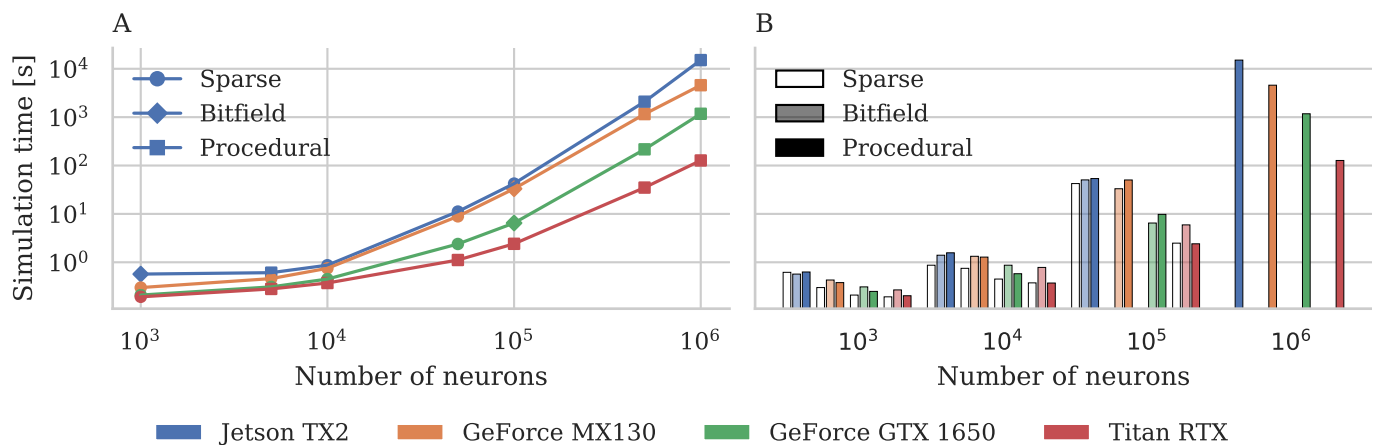PNAS | March 25, 2020 | vol. XXX | no. XX | 1–6

Fig. 1. Simulation time performance scaling on a range of modern GPUs (colors). **A** The best performing approach at each scale on each GPU (indicated by the symbols). For the largest models, the procedural method is always best. **B** Raw performance of each approach on each GPU. Missing bars indicate insufficient memory to simulate.

hardware to rapidly switch between tasks so that the latency of accessing external memory can be 'hidden' behind computation, as long as there is sufficient computation to be performed. For example, the memory latency of a typical modern GPU can be completely hidden if each CUDA core performs approximately 10 arithmetic operations per byte of data accessed from memory. Unfortunately, processing a synapse in a spiking neural network simulation is likely to require accessing approximately 8 B of memory and performing many fewer than the required 80 instructions. This makes synaptic updates highly memory bound. Nonetheless, we have shown in previous work (13) that, as GPUs have significantly higher total memory bandwidth than even the most expensive CPU, moderately sized models of around 10×10^3 neurons and 1×10^9 synapses can be simulated on a single GPU with competitive speed and energy requirements. However, individual GPUs do not have enough memory to simulate truly large-scale brain models and, although small numbers of GPUs can be connected together using the high-speed NVLink **(TODO: cite)** interconnect, beyond such small GPU clusters, scaling will be dictated by the same communication overheads as for other MPI-based distributed systems.

In this work we present a novel approach which converts large-scale brain simulation from a problem which is memory-bound on a GPU to one where the large amount of computational power available on a GPU can be used to reduce both memory and memory bandwidth requirements and enable truly large-scale brain simulations on a single GPU workstation.

Results

In the following subsections, we will first present two recent innovations in our GeNN simulator (14) which allow it to be used for simulating large-scale models on a single GPU. We will then demonstrate the power of these new features by simulating a recent model of the Macaque visual cortex (15) consisting of 4.13×10^6 neurons and 24.2×10^9 synapses on a single GPU. We find that we not only obtain the same results as in the previous simulation on a high-performance supercomputer, but our simulation also runs faster.

Procedural connectivity. The first crucial innovation to enable truly large scale simulations on a GPU is what we call 'pro-

cedural connectivity'. Our GeNN simulator (14) uses code generation to convert neuron and synapse models – described using 'snippets' of C-like code – into CUDA code for GPU simulation. We previously extended GeNN to allow the same approach to be used for generating efficient, parallel model initialisation code from code snippets describing state variable and synaptic connectivity initialisation algorithms (13). Offloading initialisation to the GPU sped up model initialisation by around $20\times$ on a desktop PC (13), suggesting that these initialisation algorithms are well-suited to GPU acceleration. **(TODO: something explaining why this is for synapses)** In fact, it seems somewhat illogical to run these algorithms only once to fill the limited memory of the GPU with data only to then read it back throughout the simulation and in so doing, overload the limited memory bandwidth. What if we could instead 'procedurally' generate connectivity and synaptic weights 'on the go' as spikes are triggered? If we could do this in less than the 80 instructions required to hide memory latency in the current approach, this new approach could be *faster* as well as requiring no memory to store connectivity and synaptic weights. Although this idea has not been previously applied to modern hardware, Eugene Izhivich used a similar approach for simulating an extremely large thalamo-cortical model with 1×10^{11} neurons and 1×10^{15} synapses on a modest PC cluster in 2005 **(TODO: cite)**. Sadly, while this remains an incredible achievement, simulating the model for 1 second of biological time required 50 days of simulation. However, high-end GPUs have thousands of times more compute power than the CPUs available in 2005 and, due to the limited memory bandwidth available to each of their parallel computing elements, are particularly well-suited to this approach.

We implemented procedural connectivity as an option for simulation runs in GeNN by repurposing our previously developed parallel initialisation methods. Instead of being run once at the beginning of the simulation, the methods are re-run during the simulation for each pre-synaptic spike until all postsynaptic targets have been identified and the postsynaptic code can be run. For instance, when connecting two populations of neurons with a fixed connections probability P_{conn}, the postsynaptic targets of a presynaptic neuron can be modelled as a Bernoulli process with success probability
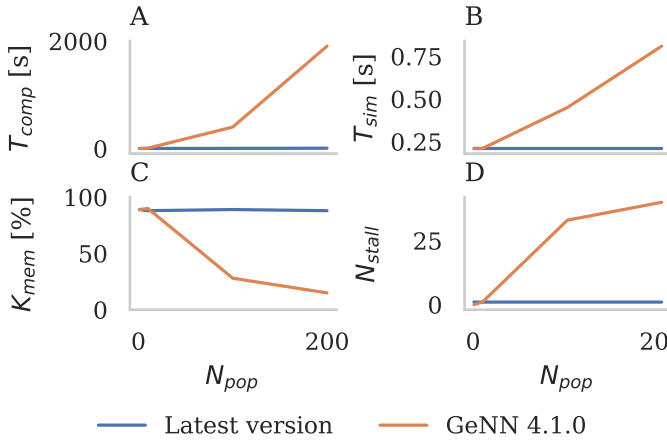
Fig. 2. Performance of a simulation of $1\,000\,000$ LIF neurons driven by a gaussian input current, partitioned into varying numbers (N_{pop}) of populations and running on a workstation equipped with a Titan RTX GPU. **A** Compilation time (T_{comp}) using GCC 7.5.0. **B** Simulation time (T_{sim}) for an 1 s simulation. **C** Memory throughput (K_{mem}) reported by NVIDIA Nsight compute profiler 'Speed of light' metric. **D** Number of 'No instruction' stalls reported by NVIDIA Nsight compute profiler (N_{stall}).

P_{conn}. An instance of the Bernoulli process can be generated by repeatedly drawing from the uniform distribution Unif$[0,1]$ and comparing each sample to P_{conn}, but this is innefficient for sparse connectivity. Instead we can sample from the geometric distribution Geom$[P_{\mathrm{conn}}]$ which is the distribution of the number of Bernoulli trials required to get a success (i.e. a synapse). The geometric distribution can be sampled in constant time by inverting the cumulative density function (CDF) of the equivalent continuous distribution (the exponential distribution) to obtain $\frac{log(\mathrm{Unif}[0,1])}{log(1-P_{\mathrm{conn}})}$ (16, p499). Therefore, as long as one has the ability to generate a unique but repeatable stream of random numbers for each presynaptic neuron, the postsynaptic targets of a presynaptic neuron can be 'procedurally' generated in parallel. **(TODO: This is confusing to me: Do you mean different pre-synaptic neurons can dice out their connections in parallel but each presyn neuron must do it in a loop, right? Am I missing something?)** While suitable random number streams *could* be provided by a 'convential' random number generator (RNG), each presynaptic neurons would need to maintain its own RNG state which would have a significant memory overhead. Instead, we use a 'counter-based' Philox4×32-10 RNG (17). Counter-based RNGs are designed for parallel applications and essentially consist of a pseudo-random bijective function which takes a counter as an input (in this case a 128 bit number) and outputs random numbers. In constrast to convential RNGs, this means that generating the nth random number in a stream has exactly the same cost as generating the 'next' random number, allowing us to trivially divide up the random number stream between multiple parallel processes (in this case presynaptic neurons). **(TODO: do we need some more explanation of how you get from this to a network simulation?)**

For an initial demonstration of the performance and scalability of procedural connectivity, we used a network that was initially designed to investigate signal propagation through cortical networks (18), but subsequently has been widely used as a scalable benchmark (19). The network consists of N integrate-and-fire neurons, partitioned into $\frac{4N}{5}$ excitatory and $\frac{N}{5}$ inhibitory neurons. The two populations of neurons are connected to each other and with themselves with a fixed $P_{\mathrm{conn}} = 10\,\%$ connection probability.

We ran simulations of this network at scales ranging from 1×10^3 to 1×10^6 neurons (corresponding to 100×10^3 and 100×10^9 synapses respectively) on a selection of modern NVIDIA GPU hardware:

Jetson TX2 a low-power embedded system designed for robotic applications with $8\,\mathrm{GB}$ of shared memory

Geforce MX130 a laptop GPU with $2\,\mathrm{GB}$ of dedicated memory

Geforce GTX 1650 a low-end desktop GPU with $4\,\mathrm{GB}$ of dedicated memory

Titan RTX a high-end workstation GPU with $24\,\mathrm{GB}$ of dedicated memory

In Fig. 1 we compare the duration of these simulations using our new procedural approach against the standard approach of storing synaptic connections in memory using two different data structures. Both data structures are described in more detail in our previous work (13) but briefly, in the 'sparse' data structure, a presynaptic neuron's postsynaptic targets are represented as a sorted array of indices whereas, in the 'bitfield' data structure, they are represented as a $N_{\mathrm{pre}} \times N_{\mathrm{post}}$ array of bits where '1' indicates the existence of a synapse and '0' its absence. None of the devices have enough memory to store the 100×10^9 synapses required for the largest scale using either data structure but, at the 100×10^3 neuron scale, the bitfield data structure allows the model to fit into the memory of several devices it otherwise would not. However, not only is the new procedural approach the *only* way of simulating models at the largest scales but, as Fig. 1 illustrates, even at smaller scales its performance is competitive with and sometime better than the standard approach. **(TODO: note that this is using synapses with fixed synaptic weight)**

Kernel merging. The second innovation we named "kernel merging" and relates to the way code is organised into CUDA kernel functions. While the procedural connectivity approach presented in the previous section allows us to simulate models which would otherwise not fit within the memory of a single GPU, there are additional problems when using code generation to generate simulation code for models with a large number of neuron and synapse populations.

GeNN and – to the best of our knowledge (20) – all other SNN simulators which use code generation to generate all of their simulation code (as opposed to, for example NESTML (21), which uses code generation to generate neuron simulation code) generate seperate pieces of code to simulate each population of neurons and synapses. This approach allows optimizations such as the hard-coding of constant parameters to be easily performed and, although generating code for models with many populations will result in large code size, C++ CPU code can be easily divided between multiple modules and compiled in parallel, minimizing the effect on build time. However, GPUs can only run a small number of kernels – which are equivalent to modules in this context – simultaneously (128 on the latest NVIDIA GPUs **(TODO: cite)**). Therefore, in GeNN, multiple neuron populations are simulated within each kernel, resulting in code of the form shown in the following pseudocode which illustrates how 3 populations of 1000 neurons could be simulated in a single kernel: **(TODO: very minimal sentance about SIMT**
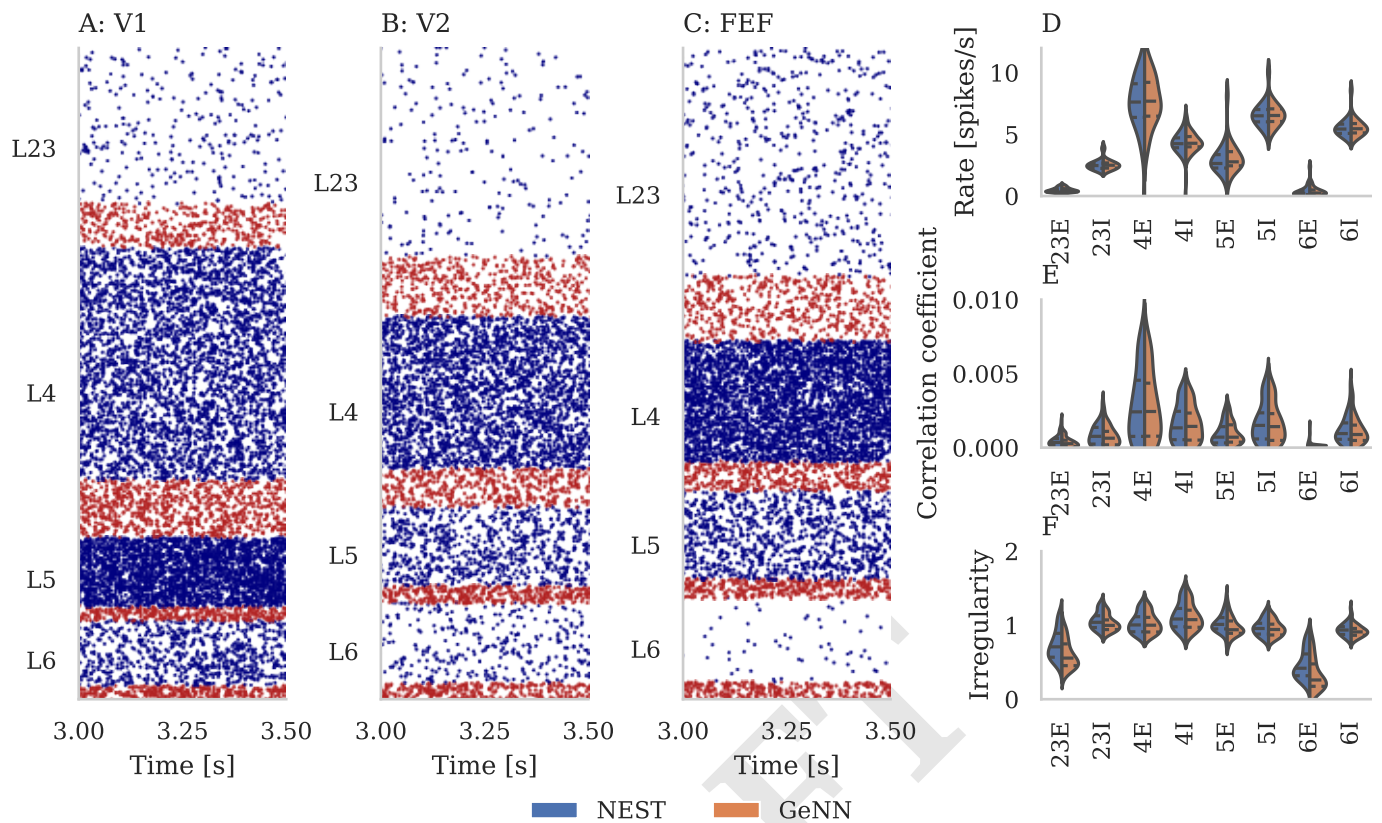
Fig. 3. Results of full-scale multi-area model simulation. **A-C** Raster plots of spiking activity of 3 % of the neurons in area V1 **A**, V2 **B**, and FEF **C**. Blue: excitatory neurons, red: inhibitory neurons. **D-F** Spiking statistics for each population across all 32 areas simulated using GeNN and NEST shown as split violin plots. Solid lines: medians, Dashed lines: Interquartile range (IQR). **D** Population-averaged firing rates. **E** Average pairwise correlation coefficients ofspiking activity. **F** Irregularity measured by revised local variation LvR (22) averaged across neurons.

here)

```
void updateNeurons()
{
    if(thread < 1000) {
        // Update neuron population A
    }
    else if(thread >= 1000 && thread < 2000) {
        // Update neuron population B
    }
    else if(thread >= 2000 && thread < 3000) {
        // Update neuron population C
    }
}
```

This approach works well for models with small numbers of populations but, as Fig. 2A illustrates, when we partition a model consisting of 1 000 000 LIF neurons into a large number of populations (increasing the size of the neuron kernel), compilation times increases super-linearly – quickly becoming impractical. Furthermore, Fig. 2B shows that when the model is partitioned into a large number of populations, the simulation also runs much more slowly. We would expect this model to be memory bound as each thread in the model reads 32 B of data and, as we discussed previously, hiding the latency of these memory accesses would require approximately 320 arithmetic operations which is many more than are required to sample from the uniform distribution and update a LIF

neuron. Fig. 2C – obtained using data from the NVIDIA Nsight compute profiler **(TODO: cite)** – shows that this to be true with the memory system being around 90 % utilised for small numbers of populations. However, when the model is partitioned into a large number of populations, the kernel stops being able to efficiently use the memory and becomes latency bound (neither memory *or* compute are used efficiently). Investigating further using the profiler showed that this drop in performance was accompanied by an increasing number of "No instruction" stalls as shown in Fig. 2D. Stalls are events which prevent the GPU from doing any work during a clock cycle and the profiler documentation suggests that these particular events are likely to be caused by "Excessively jumping across large blocks of assembly code"**(TODO: cite)** – which makes sense when we are generating kernels with hundreds of thousands of lines of code. **(TODO: is more detail required here as to why?)**

To address these issues, we developed a new code generator for GeNN which first 'merges' the model description, grouping populations which can be simulated using the same generated code. From this merged description, structures are generated to store the pointers to state variables and the parameters which can differ between merged populations:

```
struct NeuronUpdateGroup
{
    unsigned int numNeurons;
    float* V;
```

Knight *et al.*

```
293    };
```

An array of these structures is then declared for each merged population and each element is initialised with pointers to state variables and parameter values:

```
297    NeuronUpdateGroup neuronUpdateGroup[3];
298    neuronUpdateGroup[0] = {1000, VA};
299    neuronUpdateGroup[1] = {1000, VB};
300    neuronUpdateGroup[2] = {1000, VC};
```

In order for a thread to determine which neuron in which population it should be simulating, we generate an additional data structure – an array containing a cumulative sum of threads used for each population. Each thread performs a simple binary search within this to find the index of the neuron and population it should simulate:

```
307    unsigned int startThread[3] = {0, 1000, 2000};
308    void updateNeurons()
309    {
310        if(thread < 3000) {
311            // Binary search startThread to determing
312            // which population thread should be
313            // processed. Then update using variables
314            // in neuronUpdateGroup
315        }
316    }
```

As Fig. 2 shows, this approach entirely solves the issues with compilation time and simulation performance caused by large numbers of populations. Therefore, we apply this approach to initialisation and simulation kernels for both neuron and synapse populations.

The multi-area model. Due to lack of computing power and sufficiently detailed connectivity data, previous models of the cortex have either focussed on modelling individual local microcircuits at the level of individual cells (23, 24) or modelling multiple connected areas at a higher level of abstraction where entire ensembles of neurons are described by a small number of differential equations **(TODO: find citation)**. However, data from several species **(TODO: find citation)** has shown that cortical activity has distinct features at both the global and local levels which can only be captured by modelling interconnected microcircuits at the level of individual cells. The recent multi-area model (15, 25) does this – using scaled versions of a previous 4 layer microcircuit model (24) to implement $1\,\text{mm}^2$ 'patches' for each of 32 areas of the macaque cortex involved in visual processing. The 32 areas are connected together with connectivity based on inter-area axon tracing data from the CoCoMac (26) database, further refined using additional anatomical data (27) and heuristics (28) to obtain estimates for the number of synapses connecting pairs of areas. Synapses between areas are then distributed between the populations which make up each area **(TODO: finish)**. This model was simulated using NEST (2) on a single rack of a IBM Blue Gene/Q supercomputer (a 2 m high enclosure containing 1024 compute nodes and weighing over 2 t). On this system, initialization of the model took around 5 min and simulating 1 s of biological time took approximately 12 min (15).

The multi-area model consists of 4.13×10^6 neurons split into 254 populations and 24.2×10^9 synapses split into 64 516

populations meaning that, without the kernel merging approach presented earlier in this work, the model would be unlikely to compile or simulate at a reasonable speed using GeNN. Additionally, each synapse in this model has an independant weight and synaptic delay sampled from a normal distribution, meaning that the bitfield data structure cannot be used to represent the connectivity. Even if we assume that 16 bit floating point would provide sufficient weight precision, delays can be expressed as a 8 bit integer and that the neuron populations are all small enough to index using 16 bit indices, our sparse data structure would still require 5 B per synapse, meaning that this model's synaptic data would require over 100 GB. While a cluster of GPUs connected using NVLink could be built with this much memory, it is more than any single GPU has available.

In this model, the density of the synaptic connections between a pair of neuronal populations is specified in terms of a total number (N_{syn}) of random synapses. In order to use our procedural approach to simulate a model with this connectivity, the subset of the N_{syn} synapses which end up in each row must be pre-calculated by sampling from the multinomial distribution $\text{Mult}[N_{\text{syn}}, \{P_{row}, P_{row}, \dots, P_{row}\}]$ where $P_{row} = \frac{N_{\text{post}}}{N_{\text{pre}} N_{\text{post}}} = \frac{1}{N_{\text{pre}}}$. This operation cannot be efficiently parallelised so must be performed on the host but, once the length of each row is determined, the postsynaptic targets of each presynaptic neuron can be procedurally generated in parallel by sampling from the discrete uniform distribution $\text{Unif}[0, N_{\text{post}}]$. The weights and delays for each synapse generated in this manner can then be sampled from the normal distribution using the same, repeatable random number generator stream.

In order to validate our GeNN simulations of the multi-area model we ran a 10.5 s simulation of the model in the ground state on a workstation with a single Titan RTX GPU. Initialization our model took 6 min – 3 min of which was spent generating and compiling code – and each biological second of simulation took 7.7 min – Fig. 3A-C shows some example spiking activity from three of the modelled areas. Next, we compared the per-layer distributions of rates, spike-train irregularity and cross-correlation coefficients across all areas with those obtained from the supercomputer simulations. Irregularity was calculated using the revised local variaation LvR (22) averaged over a subsample of 2000 neurons and

Discussion

- Further scaling - memory only required for neuron parameters
- Learning
- Hardware for procedural connectivity?

Materials and Methods

Neuron models. The membrane voltage (V_j) of each neuron is modelled as a leaky integrate-and-fire (LIF) unit:

$$\tau_m \frac{dV_j}{dt} = (V_j - V_{rest}) + R_m I_{in_j} \qquad [1]$$

where τ_m and R_m represent the time constant and resistance of the neuron's cell membrane, V_{rest} defines the membrane voltage the neuron returns to if it receives no synaptic input and I_{in_j} represents the input current to the neuron. When the membrane voltage crosses a threshold (V_{thresh}) a spike is emitted, the membrane

voltage is reset back to V_{rest} and a countdown timer is started which, while running, disables the integration of further input thus providing a simulated refractory period. Incoming spikes induce an exponentially-shaped input current in I_{in_j}:

$$\tau_{syn}\frac{dI_{in_j}}{dt} = -I_{in_j} + I_{p_j} + \sum_{i=0}^{n} w_{ij} \sum_{t_i^f} \delta(t - t_i^f) \qquad [2]$$

where τ_{syn} represents the time constant with which any spikes (modelled as Dirac delta functions δ) from n presynaptic input neurons occuring at time t are integrated. In addition to its synaptic input, each neuron in the network also receives an independent Poisson input current I_{p_j} (also exponentially shaped by equation 2) which represents input from adjacent cortical regions.

1. Herculano-Houzel S, Mota B, Lent R (2006) Cellular scaling rules for rodent brains. *Proceedings of the National Academy of Sciences* 103(32):12138–12143.
2. Gewaltig MO, Diesmann M (2007) NEST (NEural Simulation Tool). *Scholarpedia* 2(4):1430.
3. Carnevale NT, Hines ML (2006) *The NEURON book*. (Cambridge University Press).
4. Jordan J, et al. (2018) Extremely Scalable Spiking Neuronal Network Simulation Code: From Laptops to Exascale Computers. *Frontiers in Neuroinformatics* 12(February):2.
5. Frenkel C, Lefebvre M, Legat JD, Bol D (2018) A 0.086-mmˆ2 12.7-pJ/SOP 64k-Synapse 256-Neuron Online-Learning Digital Spiking Neuromorphic Processor in 28nm CMOS. *IEEE Transactions on Biomedical Circuits and Systems* PP(XX):1–1.
6. Frenkel C, Legat Jd, Bol D (2019) A 65-nm 738k-Synapse/mm 2 Quad-Core Binary-Weight Digital Neuromorphic Processor with Stochastic Spike-Driven Online Learning in *2019 IEEE International Symposium on Circuits and Systems (ISCAS)*. (IEEE), pp. 1–5.
7. Furber SB, Galluppi F, Temple S, Plana LA (2014) The SpiNNaker Project. *Proceedings of the IEEE* 102(5):652–665.
8. Merolla PA, et al. (2014) A million spiking-neuron integrated circuit with a scalable communication network and interface. *{S}cience* 345(6197):668–673.
9. Qiao N, et al. (2015) A reconfigurable on-line learning spiking neuromorphic processor comprising 256 neurons and 128K synapses. *Frontiers in Neuroscience* 9(APR):1–17.
10. Schemmel J, Kriener L, Muller P, Meier K (2017) An accelerated analog neuromorphic hardware system emulating NMDA- and calcium-based non-linear dendrites. *Proceedings of the International Joint Conference on Neural Networks* 2017-May:2217–2226.
11. van Albada SJ, Helias M, Diesmann M (2015) Scalability of Asynchronous Networks Is Limited by One-to-One Mapping between Effective Connectivity and Correlations. *PLoS Computational Biology* 11(9):1–37.
12. Rhodes O, et al. (2019) Real-Time Cortical Simulation on Neuromorphic Hardware.
13. Knight JC, Nowotny T (2018) GPUs Outperform Current HPC and Neuromorphic Solutions in Terms of Speed and Energy When Simulating a Highly-Connected Cortical Model. *Frontiers in Neuroscience* 12(December):1–19.
14. Yavuz E, Turner J, Nowotny T (2016) GeNN: a code generation framework for accelerated brain simulations. *Scientific reports* 6(November 2015):18854.
15. Schmidt M, et al. (2018) A multi-scale layer-resolved spiking network model of resting-state dynamics in macaque visual cortical areas. *PLoS Computational Biology* 14(10):1–38.
16. Devroye L (2013) *Non-uniform random variate generation*. (Springer-Verlag New York, New York).
17. Salmon JK, Moraes MA, Dror RO, Shaw DE (2011) Parallel random numbers: As Easy as 1, 2, 3 in *Proceedings of 2011 International Conference for High Performance Computing, Networking, Storage and Analysis on - SC '11*. (ACM Press, New York, New York, USA), Vol. 81, p. 1.
18. Vogels TP, Abbott LF (2005) Signal Propagation and Logic Gating in Networks of Integrate-and-Fire Neurons. *The Journal of Neuroscience* 25(46):10786–10795.
19. Brette R, et al. (2007) Simulation of networks of spiking neurons: a review of tools and strategies. *Journal of computational neuroscience* 23(3):349–98.
20. Blundell I, et al. (2018) Code Generation in Computational Neuroscience: A Review of Tools and Techniques. *Frontiers in Neuroinformatics* 12(November).
21. Plotnikov D, et al. (2016) NESTML: a modeling language for spiking neurons. pp. 93–108.
22. Shinomoto S, et al. (2009) Relating neuronal firing patterns to functional differentiation of cerebral cortex. *PLoS Computational Biology* 5(7).
23. Izhikevich EM, Edelman GM (2008) Large-scale model of mammalian thalamocortical systems. *Proceedings of the National Academy of Sciences of the United States of America* 105(9):3593–8.
24. Potjans TC, Diesmann M (2014) The Cell-Type Specific Cortical Microcircuit: Relating Structure and Activity in a Full-Scale Spiking Network Model. *Cerebral Cortex* 24(3):785–806.
25. Schmidt M, Bakker R, Hilgetag CC, Diesmann M, van Albada SJ (2018) Multi-scale account of the network structure of macaque visual cortex. *Brain Structure and Function* 223(3):1409–1435.
26. Bakker R, Wachtler T, Diesmann M (2012) CoCoMac 2.0 and the future of tract-tracing databases. *Frontiers in Neuroinformatics* 6(DEC):1–6.
27. (2014) A weighted and directed interareal connectivity matrix for macaque cerebral cortex. *Cerebral Cortex* 24(1):17–36.
28. Ercsey-Ravasz M, et al. (2013) A Predictive Network Model of Cerebral Cortical Connectivity Based on a Distance Rule. *Neuron* 80(1):184–197.